Vapour and mechanically induced chromic behaviour of platinum complexes with a dimer-of-dimer motif and the effects of hetero metal ions

*Tadashi Ohba, Atsushi Kobayashi, Ho-Chol Chang, Masako Kato**

Supplementary Information

Contents

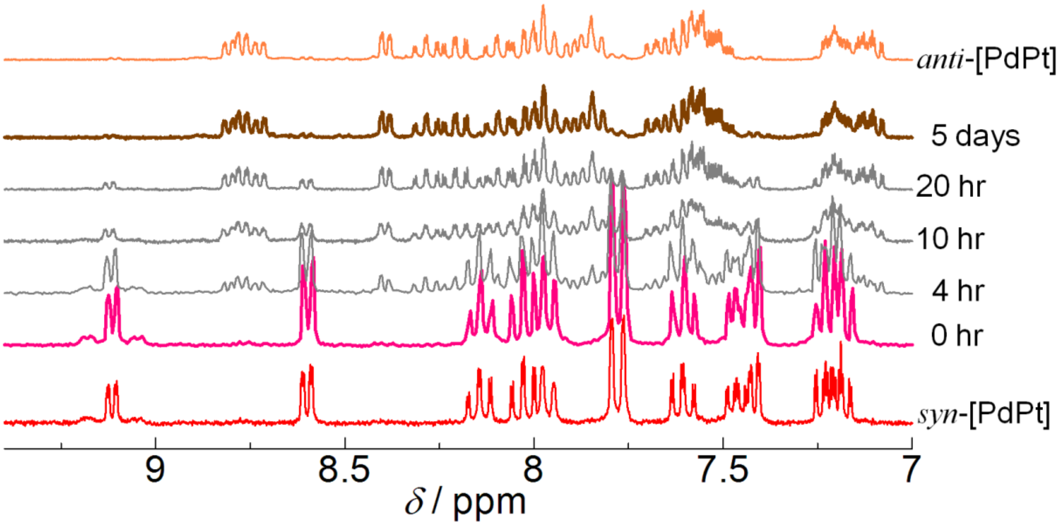

Fig. S1 ^{1}H NMR spectral changes showing the isomerization from *syn*-[**PdPt**] to *anti*-[**PdPt**] in CD_3CN (0 h – 5 d). The spectra at the top and bottom were those of crystalline samples used for X-ray analysis, *anti*-[**PdPt**] and *syn*-[**PdPt**], respectively.

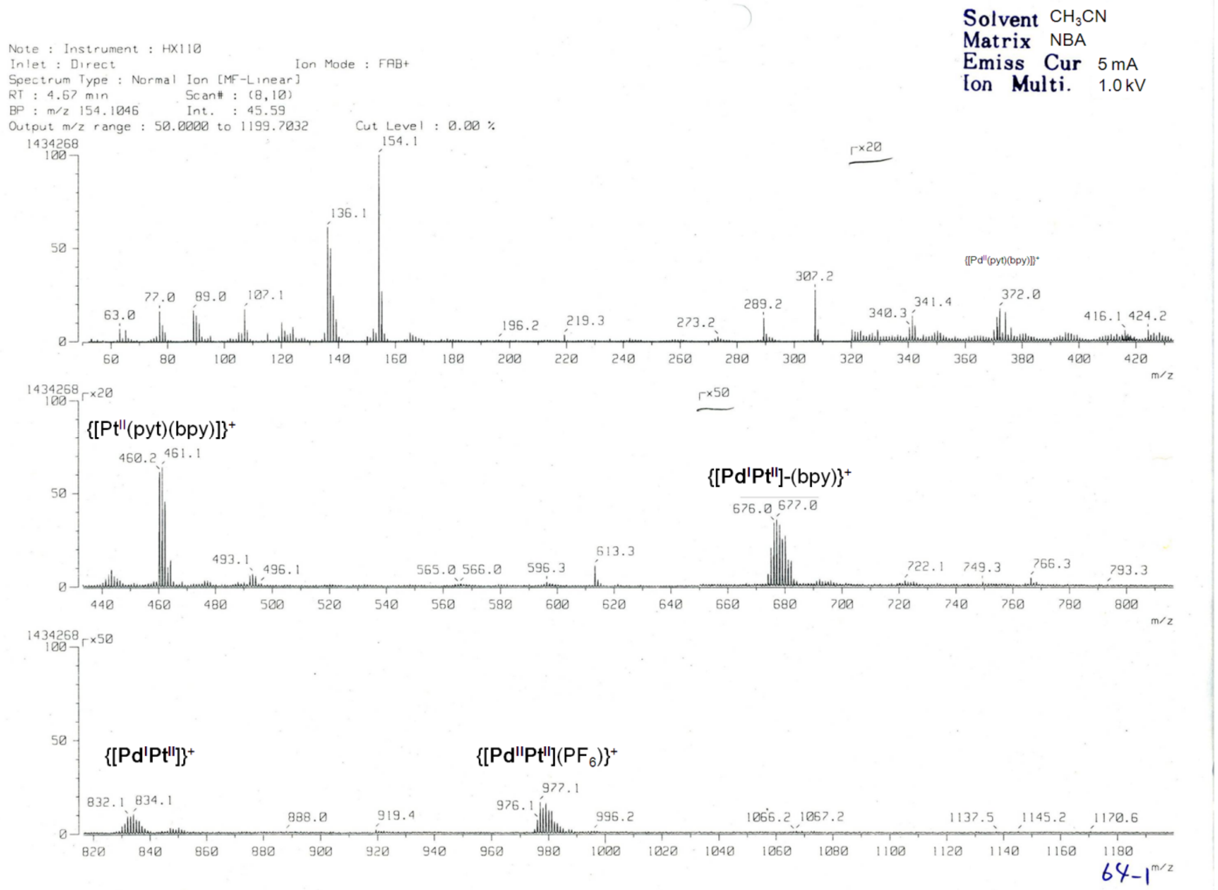
Note : Instrument : HX110
Inlet : Direct Ion Mode : FAB+
Spectrum Type : Normal Ion [MF-Linear]
RT : 4.67 min Scan# : (8,10)
BP : m/z 154.1046 Int. : 45.59
Output m/z range : 50.0000 to 1199.7032 Cut Level : 0.00 %

Solvent CH_3CN
Matrix NBA
Emiss Cur 5 mA
Ion Multi. 1.0 kV

Fig. S2. FAB-MS spectra of *anti*-[**PdPt**]$(PF_6)_2$.

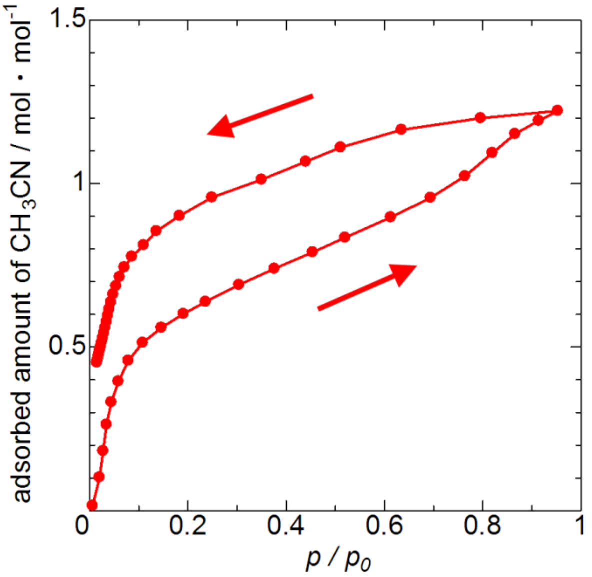

Fig. S3 CH_3CN vapour-adsorved isotherm of *syn*-[**PdPt**] at 298 K.

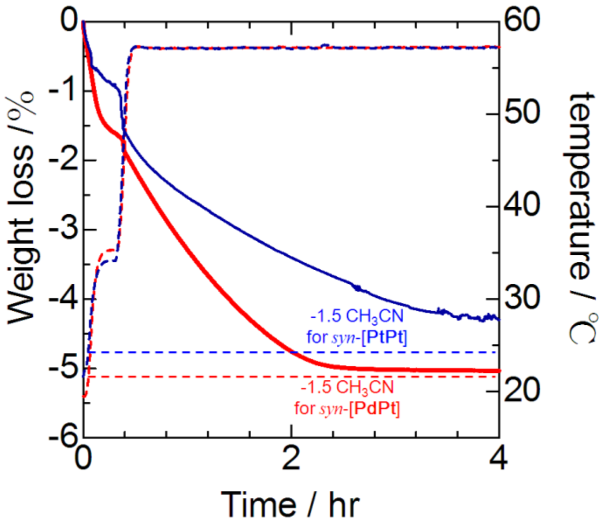

Fig. S4 Thermogravimatric analyses for the CH_3CN-included forms of *syn*-[**PdPt**] (blue) and *syn*-[**PtPt**] (red).

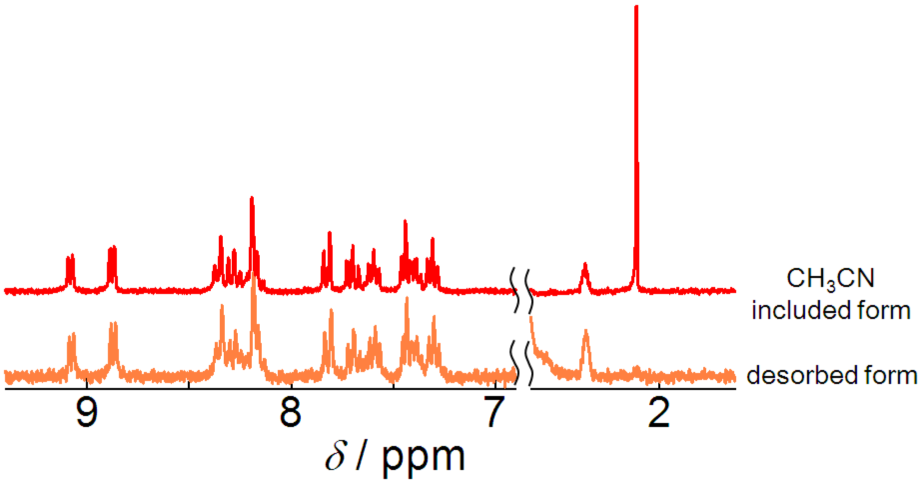

Fig. S5 ^1H NMR spectra of the red CH_3CN-included form and orange desorbed form of *syn*-[**PdPt**] in DMSO-d_6.

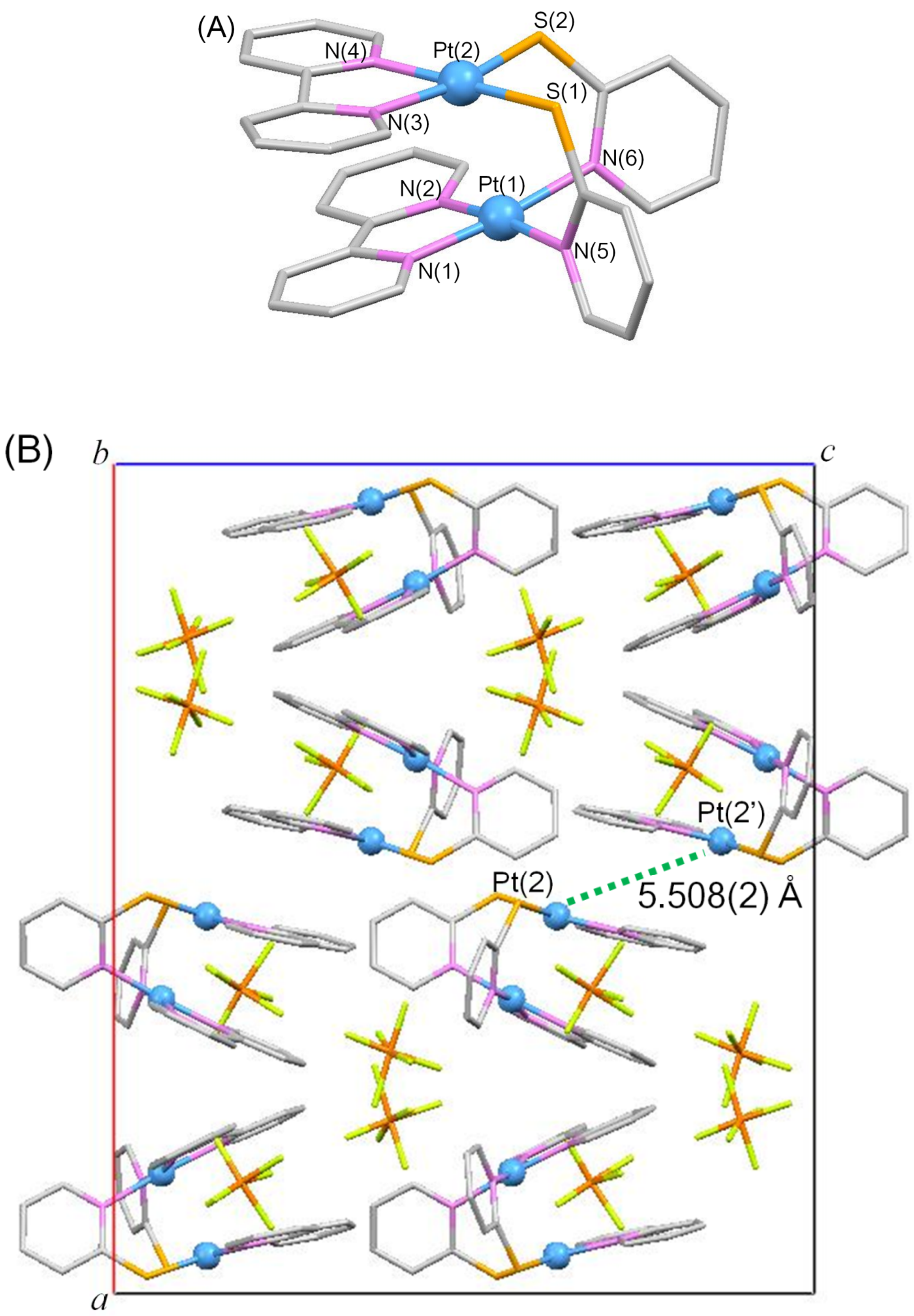

Fig. S6 (A) Molecular and (B) packing structures of the light-red form of *syn*-[PtPt](PF_6)$_2$.

Crystal data: Formula = $C_{30}H_{24}F_{12}N_6P_2S_2Pt_2$, fw = 1212.79, crystal system = orthorhombic, space group = *Pbcn* (#60), a = 25.22(2), b = 13.43(1), c = 21.32(2) Å, V = 7219(11) Å^3, T = 273 K, Z = 8, D_{calc} = 2.232 g cm^{-3}, R_1 = 0.222 ($I > 2\sigma(I)$). Pt2–S1 = 2.25(1), Pt2–S2 = 2.27(1), Pt1–N1 = 1.999(1), Pt1–N2 = 2.041(2), Pt1–N5 = 2.041(2), Pt1–N6 = 2.148(2), Pt2–N3 = 2.218(2), Pt2–N4 = 1.938(2), Pt1···Pt2 (intramolecular) = 2.876(2), Pt2···Pt2′ (intermolecular) = 5.508(2) Å

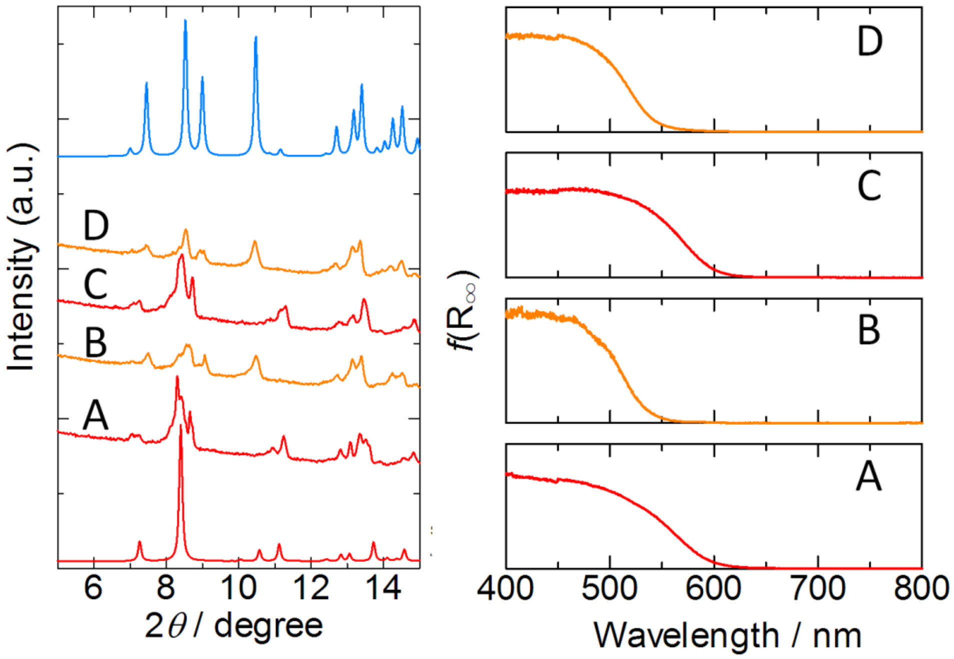

Fig. S7 Reversible vapochromic response of *syn*-**[PdPt]**. Left: The PXRD pattern changes in the repeated cycles of CH_3CN vapour exposure (A and C) and after heating at 50°C (B and D). The pattern at the bottom is for the calculated one on the basis of the single-crystal structures of the red form of *syn*-**[PdPt]** and the top pattern shows that of the light-red form of *syn*-**[PdPt]** for comparison. Right: The diffuse reflectance spectra of the samples corresponding to the PXRD data.

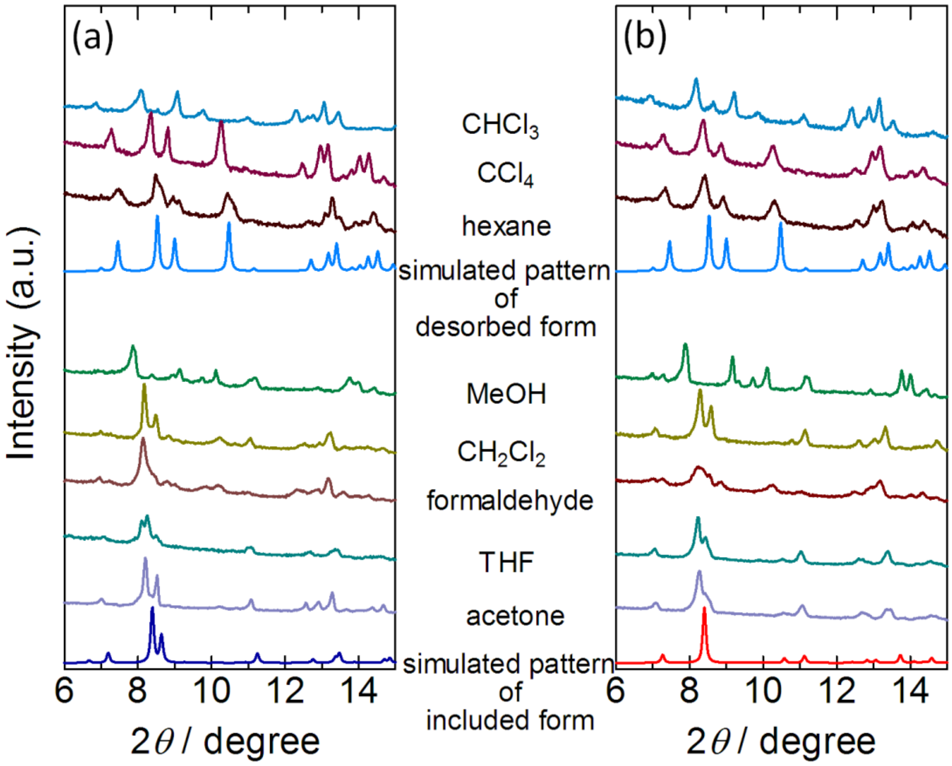

Fig. S8 PXRD patterns of (a) *syn*-[**PtPt**] and (b) *syn*-[**PdPt**] under various vapours. Exposure times were in the minutes to days range, depending on the species.

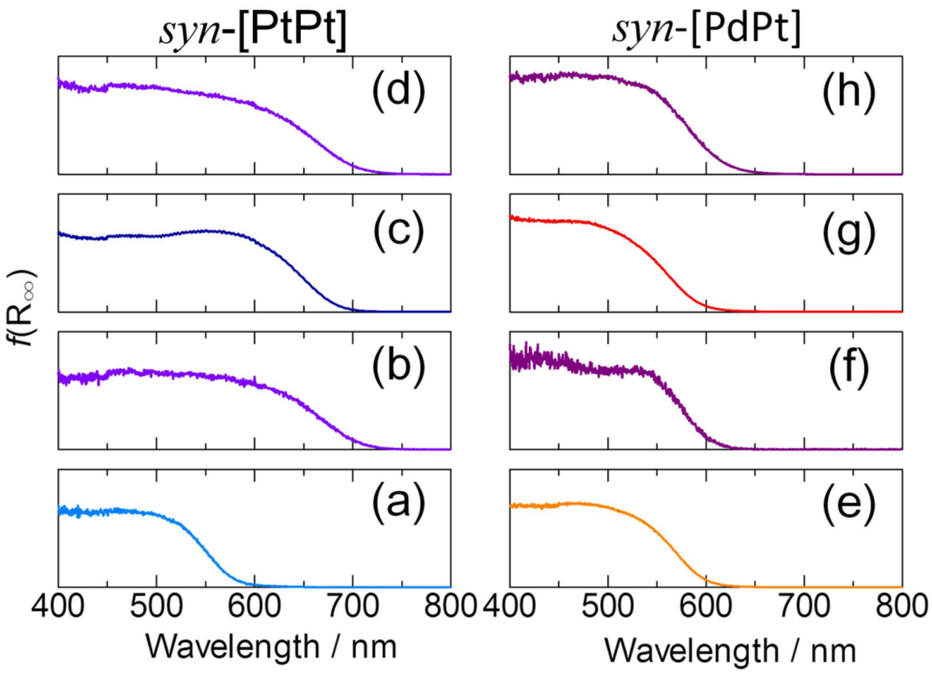

Fig. S9 UV–vis diffuse reflectance spectral changes by grinding the samples for *syn*-[**PtPt**] (a–d) and *syn*-[**PdPt**] (e–h): (a) and (e) desorbed forms (starting materials), (b) and (f) after grinding, (c) and (g) after exposure of acetonitrile vapour to ground samples, (d) and (h) re-grinding.

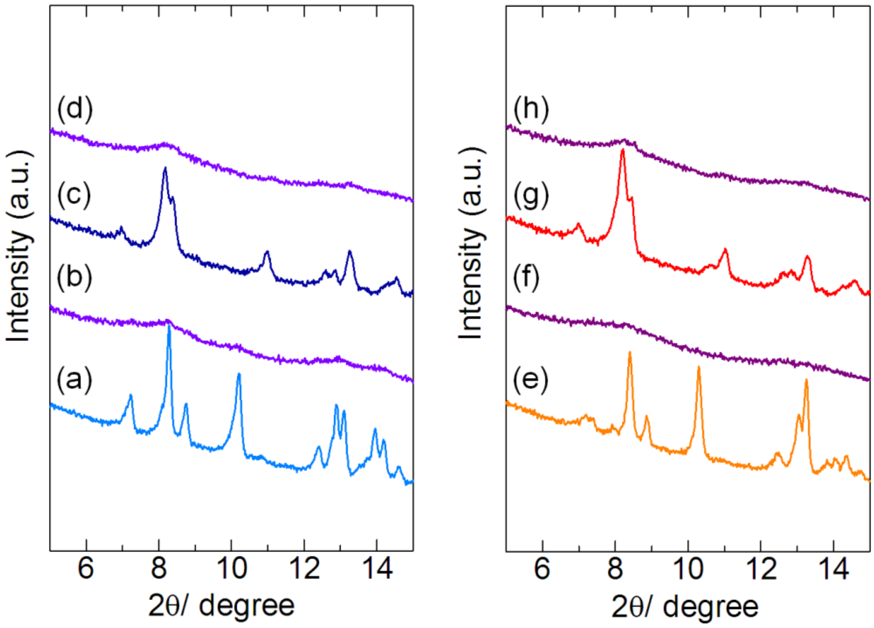

Fig. S10 Changes in PXRD patterns by grinding the samples for *syn*-[**PtPt**] (a–d) and *syn*-[**PdPt**] (e–h): (a) and (e) desorbed forms (starting materials), (b) and (f) after grinding, (c) and (g) after exposure of acetonitrile vapour to ground samples, (d) and (h) re-grinding.